Steady jets and transient jets: observational characteristics and models

M. Massi

Max Planck Institut fr̈ Radioastronomie, Auf dem Hügel 69, D-53121 Massi, Germany
e-mail: `mmassi@mpifr-bonn.mpg.de`

Abstract. Two types of radio emission are observed from X-ray binaries with jets. They have completely different characteristics and are associated with different kinds of ejections. One kind of emission has a flat or inverted spectrum indicating optically thick self-absorbed synchrotron emission; the second kind of emission corresponds to an optically thin "transient" outburst. The flat or inverted spectrum covers the whole radio band and has been established also at millimeter and infrared wavelengths. When this kind of radio emission is spatially resolved it appears as a continuous jet, the so-called "steady jet". In contrast, transient jets associated with optically thin events are resolved as "plasmoids" moving at relativistic speeds away from the center of the system. The most important point is that the two kinds of radio emission and their corresponding types of ejections seem to be related to each other; the optically thin outburst that characterizes the transient jet occurs after an interval of emission with flat/inverted spectrum. The hypothesis that the two classes of ejections correspond to two different physical processes is corroborated by X-ray observations. The transient jet is associated with the steep power-law X-ray state, whereas the continuous jet always corresponds to the low/hard X-ray state. Two different models successfully describe the two jets: a conical flow and shocks. The conical outflow describes the continuous jet and internal shocks in a continuous pre-existing outflow describe the "plasmoids" of the transient jet. The internal shocks in the outflow are thought to originate from a new population of very fast particles. Three open issues are discussed: is magnetic reconnection the physical process generating the new population of very fast particles? Is that part of the continuous jet called "core" destroyed by the transient jet and its associated shocks? Can we extrapolate these results from steady and transient jets in X-ray binaries to radio loud AGNs?

Key words. Galaxies: jets – Radio continuum: stars – Relativistic processes – X-rays: binaries – X-rays: individual: LSI+61303

1. Introduction

In the past, Seyferts galaxies, Quasars and radiogalaxies have been thought to be quite different objects, because of the quite different features observed in each of them. But later, it became clear that all of them are members of the same class, the active galactic nuclei (AGN) (Antonucci 1993), that is: supermassive black holes accreting from the host galaxy. Whereas the majority of AGNs are weak in their radio emission, about 10% are hundreds to thousands times stronger and are called "radio-loud" (Barvainis et al. 2005). The radio
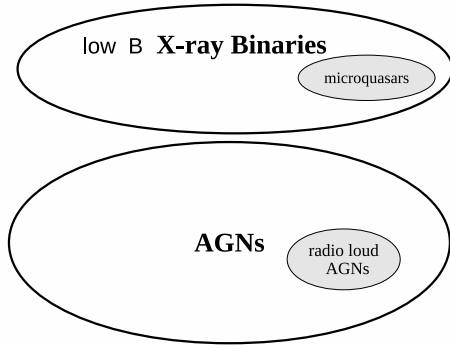
Fig. 1. Radio-emitting relativistic jets are observed in both classes of accreting compact objects: Active galactic nuclei (AGN) and low B X-ray Binaries (see text).

emission in radio-loud AGN originates from a jet.

X-ray binary systems are formed by a compact object and a normal star. X-ray binaries where the compact object is either a stellar mass black hole or a neutron star with a low magnetic field ($B \lesssim 10^8$G, Massi & Kaufman Bernadó (2008)) are the galactic equivalent to AGNs: the compact object accretes from the companion star and in some cases a radio emitting jet is observed (Fig. 1). The first X-ray binary with an associated radio jet was SS433 (Spencer 1979); in the 90's several radio-emitting X-ray binaries where discovered and named "microquasars" (Mirabel 1993).

With the seminal papers of Dhawan et al. (2000), Fender (2001) and Fender et al. (2004) it became clear that there are two different jet types: a relatively steady, continuous jet and a "transient" jet. The two types of jets have different spectral and morphological radio characteristics. In addition, when observed in X-rays the microquasars show different spectral X-ray states depending on the jet type.

Here I review these two type of jets, their different observational characteristics in radio and X-rays (Sec. 2) and their models (Sec. 3). A number of open questions are commented in Sec. 4.

2. Observational characteristics

In this section I compile different observational aspects of systems with steady or transient jets in the radio band and in X-rays. From radio observations it results that there seem to be differences in the spectral index (α), the morphology, the velocity and in polarization. X-ray differences are mainly indicated by the photon index (Γ) of the power law fitted to the spectrum.

2.1. Radio properties

The spectral index α, defined as $\alpha = \frac{log(S_1/S_2)}{log(\nu_1/\nu_2)}$, with flux density $S \propto \nu^\alpha$, is ≥ 0 in steady jets (indicating a flat or inverted spectrum) whereas in transient jets $\alpha < 0$ (see Fig. 4 in Fender (2001). The flat or inverted spectrum, $0 \leq \alpha \leq 0.6$, covers the whole radio band and has been established also at millimeter and infrared wavelengths (Fender et al. 2000; Russell et al. 2006). For transient jets the spectral index results in $-1 \leq \alpha \leq -0.2$ (Fender 2001), which corresponds to an index p=1.4−3 of the power-law energy distribution of the relativistic electrons responsible for the radio synchrotron radiation. When the radio emission corresponding to a flat/inverted spectrum is observed at high resolution it appears as a continuous jet with a bright "core" (Dhawan et al. 2000). A transient jet shows up with an optically thin radio outburst. Multifrequency radio observations of GRO J165540 show that during the radio outburst the flux densities at all observing frequencies peak simultaneously, with the amplitude of the flare increasing toward lower frequency (Hannikainen et al. 2006). At high resolution the emission is resolved in components, some time called plasmoids, movig apart (Mirabel & Rodriguez 1994; Fender et al. 1999).

The steady jet re-establishes quite soon after the optically thin outburst related to the transient jet: Dhawan et al. (2000) observed in GRS 1915+105 that the steady jet is re-established within 18 hrs from the start of a major optically thin outburst. *This implies that fast travelling components with optically thin spectrum from the transient jet may still dominate the radio emission, but in real-*
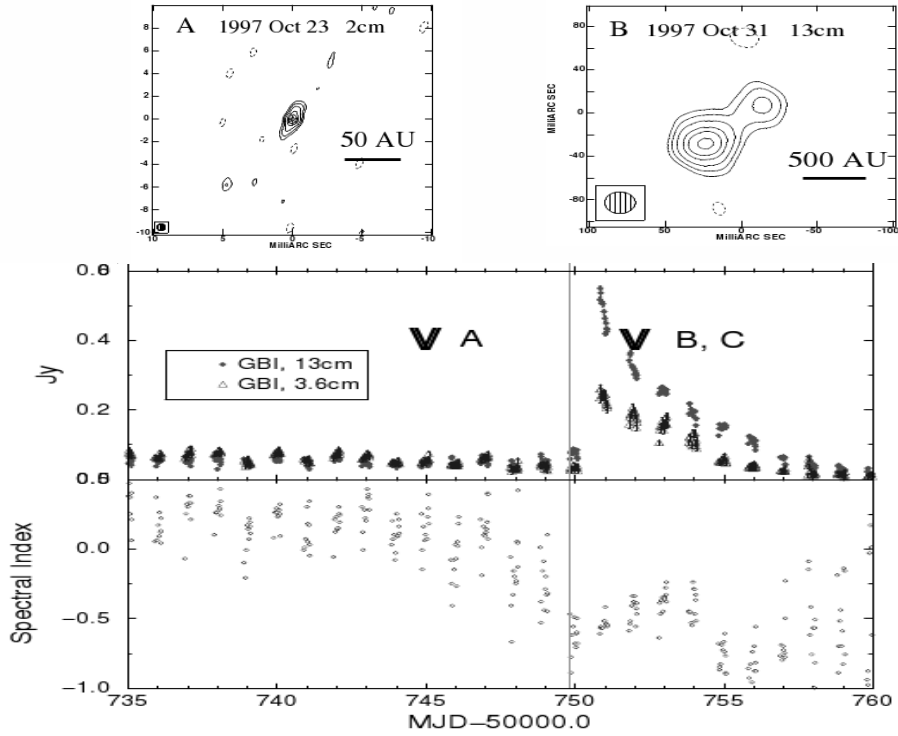
Fig. 2. Steady jet and transient jet: spectral index characteristics and morphology (Dhawan et al. (2000), reproduced by permission of the AAS).

ity they are detached from the actual situation around the engine where the steady jet re-established. Fender et al. (2004) argue that the velocities of the transient jets are significantly larger than those of the steady jets. Finally, there is evidence that the radio emission from ejected plasmoids is stronger polarized than the emission from the continuous jets (Fender & Belloni 2004).

Cygnus X-1 and GRS 1915+105 are the best examples of systems switching between the two kinds of ejections (see references in Gallo 2009). In Fig. 2, we see the transition from continuous to transient jet in spectra and morphology observed by Dhawan et al. (2000) for GRS 1915+105. In Fig. 2, one also sees that the spectrum remains flat/inverted for $\sim$ 14 days and then α switches to negative values. The outburst is optically thin, with both frequencies peaking simultaneously and

with the peak at the lowest frequency being more than a factor 2 higher than that at the higher frequency. In Fig. 2-top, simultaneous VLBA images show the continuous jet (left) and the transient jet (right). From the asymmetry between approaching and receding components of the steady jet of GRS1915+105, Dhawan et al. (2000) derived a mildly relativistic speed of $\beta = 0.1$. From the proper motion of plasmoids travelling in opposite directions from the center a high value of $\beta \geq 0.9$ was derived (Mirabel & Rodríguez 1999).

In GRS 1915+105, the continuous jet with optically thick emission corresponds to a prolonged state of relatively high, but rather stable radio emission that in fact is called "plateau". In the system LS I +61°303 , the optically thick radio emission phase corresponds to an increasing emission level, related to an increasing accretion rate, terminating in an
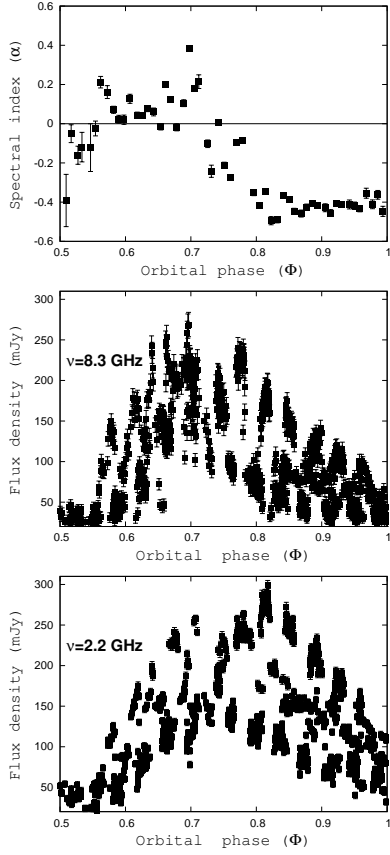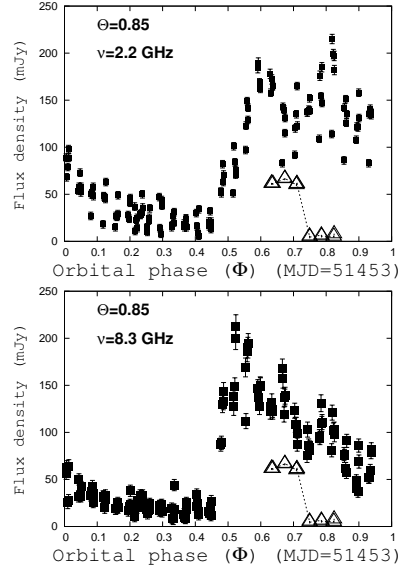
Fig. 4. Light curves of LS I +61°303 along the orbital phase at 2.2 GHz and 8.3 GHz (Massi & Kaufman Bernadó (2009), reproduced by permission of the AAS). The triangles are the Hα emission-line measurements by Grundstrom et al. (2007) multiplied here by a factor of -5 to fit in the plot.

Fig. 3. Spectral index and flux density, at 8.3 GHz and 2.2 GHz vs orbital phase, Φ (P_{orbit}=26.5 d), for Green Bank Interferometer data of the periodical source LS I +61°303 Massi & Kaufman Bernadó (2009)). The radio "outburst" is in reality formed by two consecutive outbursts: the first one optically thick (i.e. peaking at 8.3 GHz) and the second, stronger, optically thin (i.e. peaking at 2.2 GHz). Between the two outbursts there is an inversion of the spectrum from inverted to optically thin.

optically thick outburst (Bosch-Ramon et al. 2006; Massi 2010). After this inverted spectrum phase the optically thin outburst occurs as in GRS 1915+105. Figure 3 shows, folded with the orbital period of 26.5 d, light curves of LS I +61°303 at 2.2 GHz and 8.3 GHz; Figure 3-top showes the spectral index (Massi & Kaufman Bernadó 2009). At 8.3 GHz, we see a main peak of $S_{8.3GHz} = 270 \pm 15$

mJy at Φ = 0.69. We call this outburst $Peak_1$ (indicated by the vertical bar at Φ = 0.69 in Fig. 3), which is an optically thick outburst, as one can determine from the clear positive spectral index shown in the figure (Top). At 2.2 GHz, the figure shows that $Peak_1$ decays, but then the flux increases again till a large outburst at Φ = 0.82; we call this $Peak_2$ (indicated by the vertical bar at Φ = 0.82 in Fig. 3), ($S_{2.2GHz} = 299 \pm 6$ mJy). At 8.3 GHz $Peak_2$ corresponds to a minor outburst resulting in a clear optically thin spectrum.

In Fig. 4 we analyze an individual light curve (a 26 d data set). $Peak_1$ and $Peak_2$ at 2.2 GHz are well distinguishable. $Peak_1$ at 2.2 GHz (Fig. 4-Top) has a delay with respect to $Peak_1$ at 8.3 GHz (Fig. 4-Bottom), a behaviour consistent with an adiabatically expanding cloud (van der Laan 1966). Following this model, at this point an optically thin decay should follow. On the contrary at Φ = 0.8

an optically thin outburst occurs. The optically thin outburst, $Peak_2$, reaches ~220 mJy at 2.2 GHz, whereas at 8.2 GHz it is only ~130 mJy. In the same plot (Fig. 4-Bottom), are given the Hα emission-line measurements by Grundstrom et al. (2007). The Hα excess present until $\Phi = 0.71$, shows a dramatic decline at $\Phi = 0.749$ (1 day later) corresponding to the onset of the optically thin outburst.

The Hα emission line observations corroborate the scenario of two distinctly different kinds of jets, corresponding to two different underlying physical processes. Still the two jets must be related to each other: the transient jet occurs after the steady jet. We will see in Sect. 3.2 how in fact the shock-in-jet model assumes for the transient jet a pre-existing (to the transient) slow flow (i.e. the steady, continuous jet).

2.2. X-ray properties

Fender et al. (2004) pointed out, how the two different types of radio jets correspond to two different X-ray spectral states. When the microquasar showes a steady jet, its X-ray spectral state is the low/hard state corresponding to a power-law with photon index $\Gamma \sim 1.7$ (2-20 Kev) (McClintock & Remillard 2006). The optically thin radio outburst (i.e. the transient jet) is always associated with the Very High State (VHS)(Fender et al. 2004). The power-law characteristic for this state has a photon index $\Gamma \sim 2.5$ and extends into the gamma-ray regime. The VHS was renamed steep power-law X-ray state, because monitoring programs of *RXTE* showed that an unbroken steep power-law is the fundamental property of the state (McClintock & Remillard 2006). Figure 5 resumes the characteristics of these X-ray states. Fender et al. (2004) stated that it may be exactly the point of the transition to the steep power-law state that corresponds to the optically thin radio outburst.

3. Models

In this section, I briefly review the two models that describe the two jets: a conical outflow

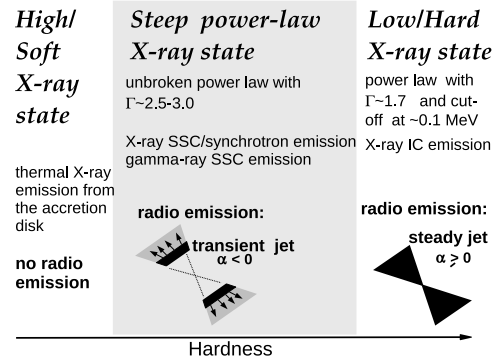| *High/ Soft X-ray state*	*Steep power-law X-ray state*	*Low/Hard X-ray state*
	unbroken power law with Γ~2.5-3.0	power law with Γ~1.7 and cut-off at ~0.1 MeV
thermal X-ray emission from the accretion disk	X-ray SSC/synchrotron emission gamma-ray SSC emission	X-ray IC emission
no radio emission	radio emission: transient jet $\alpha < 0$	radio emission: steady jet $\alpha \gtrsim 0$

Hardness

Fig. 5. X-ray spectral states and related radio states (see Massi & Zimmermann (2010), reproduced with permission ©ESO).

for the continuous jet and internal shocks in a continuous flow for the transient jet.

3.1. Conical jet

The formation of the steady jets is thought to be mediated by large-scale open magnetic fields threading the rapidly rotating accretion disks (Blandford & Payne 1982). A magnetized plasma containing energetic electrons with a power law energy distribution will produce a synchrotron power-law spectrum. However, below a critical frequency (ν_{break}), the radiating electrons will re-absorb some of the photons and as a result the typical spectrum of a uniform synchrotron source shows a peak at ν_{break}. Changes in the electron energy distribution and the decay of the magnetic field along a conical jet imply that the critical frequency varies along the jet. Assuming several jet segments (Fig. 6, see also Fig. 1 in Marscher (1995)), each producing a spectrum with a different ν_{break}, the composite spectrum will appear flat (Kaiser 2006). In microquasars, the ν_{break} for the part of the steady jet closest to the engine (i.e. ν_{break_1}) is in the infrared (Russel et al. 2010 and references there). In AGNs the observed turnover is at $10^{11\pm0.5}$ Hz, called "millimeter-wave core" in the literature (Marscher 1995). Imaging a steady jet, gives rise to the effect known as "core shift", with the shift as a function of the observing fre-

quency ν_{obs}. At ν_{obs} the emission of the segment will dominate, whose spectrum peaks at that frequency plus small contributions from neighboring segments (see Fig.1 in Markoff (2010)). Daly & Marscher (1988) calculated that changes due to the external pressure lead the jet boundary to oscillate as the jet gas periodically overexpands and reconverges in its attempt to match the ambient pressure. This effect of the boundary creates a network of waves in the interior of the jet that, converging toward the axis, may form a standing shock. Very recently, Jorstad et al. (2010) established that the millimeter-wave core in AGNs is a physical feature of the jet, i.e. coincident with the standing shock, that is different from the observed cm-wave core, the location of which is determined by the above discussed jet opacity.

Models of the low/hard X-ray state for X-ray binaries give a geometrically thin, optically thick accretion disk truncated at $R_{tr} \simeq 100 r_g$ (McClintock & Remillard 2006; Done & Diaz Trigo 2010). Following Meier (2005), the terminal velocity of the steady jet is approximately equal to the escape speed at the footpoint of the magnetic field where the jet is launched. For the large $R_{tr} \simeq 100\ r_g$ the escape velocity drops to values below 0.6 c in agreement with the low velocities inferred for steady jets. When a system is in a very low low/hard state, the even larger truncated radius may result in a very low velocity (e.g. 0.06 ± 0.01 for LS I +61°303, Peracaula et al. (1998); Massi & Zimmermann (2010)). The steady jet model therefore assumes that the flat/inverted spectrum could be the result of the variation of the magnetic field and the density of relativistic particles along a conical jet; the velocity is low for jets anchored at the large truncated radii associated to the low/hard state.

3.2. The shock-in-jet model

Fender et al. (2004) associate the change in the radio spectrum - from optically thick to optically thin - to the parallel change that is observed in the X-ray states of these sources, when passing from the low/hard X-ray state to the steep power-law state. Fender and collaborators make the hypothesis that in such a pas-
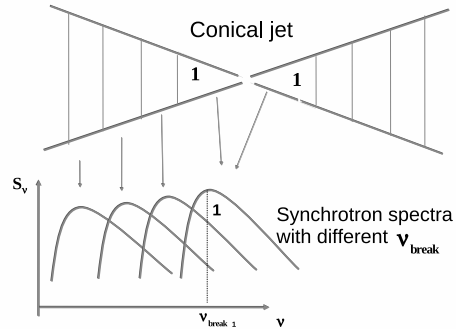

Fig. 6. Composite flat spectrum as a result of superposition of individual spectra associated at different jet segments, each with a different ν_{break}.

sage there is an increase in the bulk Lorentz factor of the ejected material. *This increase gives rise to shocks where the new highly-relativistic plasma catches up with the pre-existing slower-moving material of the steady jet.* This model, the shock-in-jet model, was originally derived by Marscher & Gear (1985) for AGNs, then generalized by Valtaoja et al. (1992); Türler et al. (2000), and introduced in the context of X-ray binaries for GRS 1915+105 by Kaiser et al. (2000) (see the review by Türler (2010)).

In the internal shock model, variations of the jet velocity or pressure lead to the formation of shock waves and electrons are accelerated. All frequencies will peak simultaneously. However, the higher energy emission particles die out first and the highest frequency emission remains confined to a thin layer behind the shock front (Fig. 7) (Marscher 2009). The width of the emission layer behind the shock front, x, is inversely proportional to the square root of the radiated frequency. As a result the flare will dominate at lower frequencies resulting in the observed optically thin outburst.

4. Discussion

I comment here on three open questions.

1. The transient jet is associated to shocks produced by differences in flow speed. For the internal shock scenario to be working and
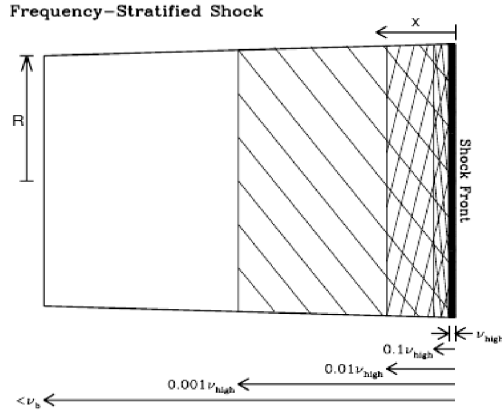
Frequency-Stratified Shock

Fig. 7. Frequency distribution behind the shock front (Marscher 2009)

giving rise to the bright optically thin radio flare (associated to shocks), particles (i.e. a new population) must be travelling with a higher velocity with respect to the preexisting low/hard state continuous flow. What kind of process can generate these fast particles? Moreover, a related open issue is the puzzling rather short timescale involved. The low/ hard phase is a relatively long and stable phase, lasting tens of days. Belloni (2005) analysed in X-rays in great detail the point of the transition from the low/hard state, distinguishing between before and after the jet line (i.e. when the transient jet is generated) into two additional states - called hard intermediate state (HIMS) and soft intermediate state (SIMS). They noticed, how sharp the transition can be, sometimes over only a few seconds (Motta et al. 2009). One kind of energy that can be built up and accumulated over long time scales and then dissipated over very short time scales clearly is magnetic energy, as we see in solar flares (Komissarov et al. 2007). Furthermore, also as in solar flares, magnetic reconnection can accelerate particles to relativistic velocities. Therefore, magnetic reconnection would be, on the basis of these two arguments, timescales and production of fast particles, a quite good candidate for triggering the transition. As a matter of fact, the prolonged removal of angular momentum from the accretion disk via the steady jet

has a very important effect on the overall process of the accretion process. As proved for the bipolar outflows from young stellar objects, the jets are capable of extracting two thirds or more of the excess angular momentum present in the disk (Woitas et al. 2005). This loss of angular momentum slows down the disk material to sub-Keplerian rotation and therefore the disk matter can finally accrete onto the central object (Matsumoto et al. 1996). This increase in accreted matter onto the compact object implies that the material pulls the deformed magnetic field with it even further. The magnetic field compression is thus increased and magnetic reconnection may occur (Novikov & Thorne 1973; Matsumoto et al. 1996; de Gouveia dal Pino 2005). In addition, as observed in the Sun, energy released during magnetic reconnection goes into electron acceleration, but in some cases also into bulk motion, propelling a flux rope away, as it occurs in a coronal mass ejection (CME) (Qiu et al. 2004). Yuan et al. (2009), in analogy with the solar CMEs, propose a magnetohydrodynamical model for transient jets, where the readjustment of the magnetic field provides the free energy to drive CME-like ejections of plasmoids. Yuan et al. (2009) suggest that the interaction of plasmoids, ejected at very highspeed, with the slow preexisting continuous jet could lead to a shock formation. Following Yuan et al. (2009) the expansion of the plasmoid would create delayed peaks in the light curves at different wavelengths as indeed observed in LS I +61°303 (Fig. 4) and in GRS 1915+105 by Mirabel et al. (1998). In addition, radio emission associated to some CME has been succesfully modelled as synchrotron radiation. Bastian (2007), analizing a radio burst associated to a CME, reproduced the drift to lower frequencies with time of the flux maximum by assuming a decrease of magnetic field and particle density due to source expansion.

2.   Observations of GRS 1915+105 by Mirabel & Rodríguez (1999) (their Fig. 2, especially the map of April 30) and by Fender et al. (1999) (their Fig. 2, especially epoch 736.7), showing moving components/shocks, seem to lack emission from

the center. Is the core destroyed by the transient? The lack of a standing shock could find an explanation in the changed conditions during the first phase of the shock and probably of broken symmetry of the conical jet. In the AGN NRAO 150 there is a sequence of observations at 86 GHZ and at 43 GHz by Agudo et al. (2007) (their Figure 3) showing that associated to the onset of fast moving components there are pronounced dips in the core light curve. At one epoch, 2006.22, rather than only a dip there seems to be a real lack of the core; this lack is confirmed also by the presented sequence of images. Agudo et al. (2007) suggest a possible change of Doppler boosting factors to explain this puzzling dip. However, the comparison with the microquasar GRS 1915+105 might suggest the alternative hypothesis that the dip could be a real one and that the core is, for a short interval, missing.

3. The above comparison between GRS 1915+105 and NRAO 150 shows how important it would be to extrapolate the knowledge on steady and transient jets in microquasars to AGNs. A comparison between the two kinds of classes presents obvious difficulties. Jets in microquasars are of the order of hundreds of AU: the relationship between jet variations and activity in the core is streightforward. In AGNs the distant jet components may be completly detached from the present activity of the core. In AGNs the steady jet remains visible under/around the shocked regions: one observes a sequence of bright and typically optically thin regions that move at superluminal speeds, embedded in the steady jet, which is in the AGN community called "underlying flow". Still, besides these difficulties, there exist several interesting parallels among the two classes of objects (Körding et al. 2006; Uttley 2006; Camenzind 2008). Radio quiet quasars would correspond to the thermal state (Fig. 5), BL LAcs and FR-I radio galaxies to the low/hard state and finally the transient jet, or steep power-law state would correspond to the FR-II radio galaxies.

References

Agudo, I., et al. 2007, A&A, 476, L17

Antonucci, R. 1993, ARA&A, 31, 473

Barvainis, R., Lehár, J., Birkinshaw, M., Falcke, H., & Blundell, K. M. 2005, ApJ, 618, 108

Bastian, T. S. 2007, ApJ, 665, 805

Belloni, T. 2005, Interacting Binaries: Accretion, Evolution, and Outcomes, 797, 197

Blandford, R. D., & Konigl, A. 1979, ApJ, 232, 34

Blandford, R. D., & Payne, D. G. 1982, MNRAS, 199, 883

Bosch-Ramon, V., Paredes, J. M., Romero, G. E., & Ribó, M. 2006, A&A, 459 , L25

Camenzind, M. 2008, MmSAI, 79, 1046

Daly, R. A., & Marscher, A. P. 1988, ApJ, 334, 539

Dhawan, V., Mirabel, I. F., & Rodríguez, L. F. 2000, ApJ, 543, 373

Dhawan, V., Mirabel, I. F., & Rodríguez, L. F. 2001, ApSSS, 276, 107

Dhawan, V., Muno, M., & Remillard, R. 2005, ASP Conference Proceedings, 340, 276

Done, C., & Diaz Trigo, M. 2010, MNRAS, 407, 2287

Fender, R. P., Garrington, S. T., McKay, D. J., Muxlow, T. W. B., Pooley, G. G., Spencer, R. E., Stirling, A. M., & Waltman, E. B. 1999, MNRAS, 304, 865

Fender, R. P., Pooley, G. G., Durouchoux, P., Tilanus, R. P. J., & Brocksopp, C. 2000, MNRAS, 312, 853

Fender, R. P. 2001, MNRAS, 322, 31

Fender, R. P., Gallo, E., & Jonker, P. G. 2003, MNRAS, 343, L99

Fender, R. P., Belloni, T. M., & Gallo, E. 2004, MNRAS, 355, 1105

Fender, R., & Belloni, T. 2004, ARA&A, 42, 317

Grundstrom, E. D., et al. 2007, ApJ, 656, 437

de Gouveia dal Pino, E. M. 2005, in Magnetic Fields in the Universe: From Laboratory and Stars to Primordial Structures, AIP Conference Proceedings, 784, 183

Hannikainen, D. C., Wu, K., Stevens, J. A., Vilhu, O., Rodriguez, J., Hjalmarsdotter, L., & Hunstead, R. W. 2006, Chinese Journal of Astronomy and Astrophysics Supplement, 6, 010000

Hannikainen, D. C. 2010, MmSAI, 81, 308

Hjellming, R. M., & Rupen, M. P. 1995, Nature, 375, 464

Kaiser, C. R., Sunyaev, R., & Spruit, H. C. 2000, A&A, 356, 975

Komissarov, S. S., Barkov, M., & Lyutikov, M. 2007, MNRAS, 374, 415

Körding, E. G., Jester, S., & Fender, R. 2006, MNRAS, 372, 1366

Jorstad, S. G., et al. 2010, ApJ, 715, 362

Markoff, S. 2010, Lecture Notes in Physics, Berlin Springer Verlag, 794, 143

Marscher, A. P. 2009, arXiv:0909.2576

Marscher, A. P., & Gear, W. K. 1985, ApJ, 298, 114

Marscher, A. P. 1995, Proceedings of the National Academy of Science, 92, 11439

Massi, M. 2010, arXiv:1009.2016

Massi, M., & Kaufman Bernadó, M. 2008, A&A, 477, 1

Massi, M., & Kaufman Bernadó, M. 2009, ApJ, 702, 1179

Massi, M., & Zimmermann, L. 2010, A&A, 515, A82

Matsumoto, R., Uchida, Y., Hirose, S., et al. 1996, ApJ, 461, 115

Meier, D. L. 2005, Ap&SS, 300, 1-3, pp. 55-659

McClintock, J. E., & Remillard, R. A. 2006, *Compact stellar X-ray sources*, Cambridge University Press, p. 157

Mirabel, I. F. 1993, Texas/PASCOS '92: Relativistic Astrophysics and Particle Cosmology, 688, 581

Mirabel, I. F., Dhawan, V., Chaty, S., Rodriguez, L. F., Marti, J., Robinson, C. R., Swank, J., & Geballe, T. 1998, A&A, 330, L9

Mirabel, I.F., & Rodríguez, L.F. 1994, Nature, 371, 46

Mirabel, I. F., Rodríguez, L. F., 1999, ARA&A, 37, 409

Motta, S., Belloni, T., & Homan, J. 2009, MNRAS, 400, 1603

Novikov, I. D., & Thorne, K. S. 1973, Black holes (Les astres occlus), p. 343

Peracaula, M., Gabuzda, D. C., & Taylor, A. R. 1998, A&A, 330, 612

Qiu, J., Wang, H., Cheng, C. Z., & Gary, D. E. 2004, ApJ, 604, 900

Remillard, R. A., & McClintock, J. E. 2006, ARA&A, 44, 49

Russell, D. M., Fender, R. P., Hynes, R. I., Brocksopp, C., Homan, J., Jonker, P. G., & Buxton, M. M. 2006, MNRAS, 371, 1334

Russell, D. M., Fender, R. P., & Jonker, P. G. 2007, MNRAS, 379, 1108

Spencer, R. E. 1979, Nature, 282, 483

Türler, M., Courvoisier, T. J.-L., & Paltani, S. 2000, A&A, 361, 850

Türler, M. 2010, arXiv:1010.0907

Uttley, P. 2006, Blazar Variability Workshop II: Entering the GLAST Era, 350, 98

Valtaoja, E., Terasranta, H., Urpo, S., Nesterov, N. S., Lainela, M., & Valtonen, M. 1992, A&A, 254, 71

van der Laan, H. 1966, Nature, 211, 1131

Woitas, J., Bacciotti, F., Ray, T. P., et al. 2005, A&A, 432, 149

Yuan, F., Lin, J., Wu, K., & Ho, L. C. 2009, MNRAS, 395, 2183